Analysis and modelling of calendar ageing in second-life lithium-ion batteries from electric vehicles

Elisa Braco, Idoia San Martín, Pablo Sanchis, Alfredo Ursúa
Dept. of Electrical, Electronics and Communications Engineering
Institute of Smart Cities. Public University of Navarre (UPNA)
Campus de Arrosadia, 31006, Pamplona, Spain
elisa.braco@unavarra.es, idoia.sanmartin@unavarra.es, pablo.sanchis@unavarra.es, alfredo.ursua@unavarra.es

***Abstract*—The reuse of Li-ion batteries from electric vehicles is a promising alternative to recycling nowadays. However, the technical and economic viability of these second-life (SL) batteries is not yet clear. Degradation assessment plays a key role not only to analyse the impact of ageing factors in reused batteries, but also to quantify their durability. In this context, this contribution aims to analyse calendar ageing behaviour in SL cells. 16 reused Nissan Leaf modules are aged during 750 days under three temperatures and four State of Charge (SOC), covering a State of Health range from 72.2 % to 13 %. The impact of temperature and SOC as stress factors is firstly analysed, concluding that their increase accelerates ageing. Temperature rise is found to have a major impact, accelerating up to 27 times capacity fade and almost 6 times resistance increase when compared to light ageing conditions, while increasing SOC nearly doubles ageing rates. The worst ageing case is found to be the combination of 60 °C and 66 % of SOC. Regarding degradation trends, they are proven to be constant during all SL lifetime. This work also proposes and validates a calendar ageing model for SL cells. Accuracy of validation results show a fitting Rsq of 0.9941 in capacity fade and 0.9557 in resistance increase, thereby tracking the heterogeneous degradation of the SL cells under calendar ageing.**

***Index Terms*—Calendar ageing, Modelling, Second-life batteries, Li-ion batteries, Electric vehicles**

I. Introduction

Electric Vehicle (EV) is a major player in automotive and energy industries nowadays. As a consequence, the demand of Li-ion batteries for EV usage is rising year on year, with values up to 160 GWh in 2020 [1].

Due to their usage, energy and power capabilities of Li-ion batteries fade, in such a way that automotive standards set 20 % of capacity loss as withdrawal point from EVs. As an alternative to direct recycling, the reuse of these batteries has emerged as a solution in recent years which allows to enlarge lifetime, thereby representing a beneficial solution both in an economic and environmental perspective [2]. Stationary applications such as residential storage or integration of renewable energies have been identified as promising uses for these second-life (SL) batteries [3], in a market which is expected to exceed 260 GWh per year by 2030 [4]. Nevertheless, the technical and economic viability of this SL use of EV batteries is still uncertain. In recent years, several contributions have assessed the performance of SL cells and modules [5]–[7], as well as of battery packs [8], with promising results.

In this context, degradation is a hot spot regarding SL viability. Battery ageing is classified in two main types: cycling and calendar. While the first type of ageing is related to battery usage, calendar degradation is a consequence of time lapse. Parasitic side reactions between electrodes and electrolyte caused by thermodynamic instability of materials are behind this degradation type, which results in capacity and power fade in Li-ion cells [9]–[11]. The main factors that contribute to calendar ageing are storage temperature and voltage, given that they accelerate parasitic reaction rates and instability of electrodes [11], [12]. The impact of these factors depends though on the specific chemistry [13], [14].

Calendar ageing has been assessed in different cells and chemistries in literature [11], but despite its importance it has been rarely reported in SL batteries. In [9], new LFP cells were aged over the SL withdrawal point until up to 50 % of their initial capacity value. However, no references to modules previously used in EVs have been found. After the performance assessment of SL Nissan Leaf modules under cycling ageing carried out in previous works [7], [15], this contribution aims to cover the gap of calendar ageing in reused cells. The specific impact of ageing factors or the durability of SL cells, given their previous usage in EVs, are some of the questions targeted.

The work is organized as follows. Section II describes the experimental setup, covering the SL modules under study, the tests performed and the bench used. The main results of this work are gathered in Section III. An insight in the influence of the ageing factors is presented in Section IV, together with the proposal and validation of a calendar ageing model. Finally, Section V gathers the main conclusions of the work.

We would like to acknowledge the support of the Spanish State Research Agency (AEI) grant PID2019-111262RB-I00/AEI/10.13039/501100011033, the European Union H2020 Project STARDUST (74094) and the Government of Navarre Ph.D. scholarship.

II. Experimental setup

A. Module description

The experimental procedure of this contribution was carried out with reused Li-ion modules from Nissan Leaf EVs. Four pouch-type cells of LMO/LNO cathode and graphite anode compose each module, associated in series-connected pairs (2s2p). Each module has three external terminals, in such a way that a 2p cell pair is the smallest testing unit available. Fig. 1 pictures some of the SL Nissan Leaf modules under test. The nominal capacity of the modules is 66 Ah, and their maximum, minimum and nominal voltages are 8.3 V, 5 V, and 7.5 V, respectively.

B. Experimental procedure description and test bench

All the experimental procedures of this contribution are carried out at 2p cell level, which will hereinafter be named as cell to ease reading. Two main experimental sets are carried out: reference performance tests (RPTs) and calendar ageing tests.

a) Reference performance tests: RPTs consist of a sequence of capacity and DC internal resistance (DCIR) measurements at a controlled ambient temperature of 25 °C. The cell is set at rest during two hours to reach thermal equilibrium. Then, it is discharged with a constant current (CC) pulse at C/3 until its minimum voltage. C is defined according to the nominal capacity of the cell, thus being 66 A. The capacity test consists of two full cycles at C/3 with constant current-constant voltage (CCCV) charge and CC discharge within cell voltage limits, considering C/30 as cut-off current of the CV phase. The capacity of the cell (C_{RPT}) is defined as the discharged capacity of the second cycle. C/3 is selected as a recommended rate not to distort results with cycling during the test [10]. Then, the cell is fully charged at C/2, and DCIR measurements are performed at SOC levels of 90 %, 70 %, 50 %, 30 % and 10 %. To reach the specific SOC, the cell is discharged with a CC pulse at C/2. After a one-hour rest, DCIR is measured as the difference between the discharge voltage and current after 10 seconds and the ones tracked at the end of the rest period.

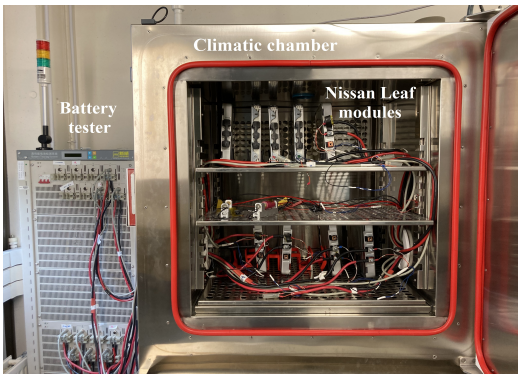

Fig. 1. Experimental setup with some of the SL Nissan Leaf modules and test bench.

b) Calendar ageing tests: Calendar ageing in Li-ion cells is mainly conditioned by storage temperature (T_{cal}) and SOC (SOC_{cal}). Given the non-linear influence of such factors in lifetime, at least three stress levels are considered. Thereby, the testing matrix covers T_{cal} values of 25 °C, 45 °C and 60 °C and SOC_{cal} values of 0 %, 33 %, 66 % and 100 %. One sample is used on each condition except at 60 °C, in which two cells are used for each SOC_{cal}. Thereby, the testing batch is formed by 16 SL cells. Cells are stored at the corresponding SOC_{cal} and T_{cal} conditions in the climatic chambers, and every 4 weeks an RPT is performed. After the RPT, the cell is fully charged at C/3 with CCCV procedure to the corresponding SOC_{cal}, considering Ah counting and C_{RPT}.

The test bench used consists of a battery tester and three climatic chambers. Fig. 1 shows the tester and one of the chambers during an RPT. The battery tester is rated at 5 V and 50 A on each channel, with an accuracy within ±0.1 % of the full scale. The climatic chambers allow a temperature range from -30 °C to +180 °C, with measurement precision of ±0.5 °C.

III. Calendar ageing experimental results

As a consequence of ageing, energy and power capabilities of Li-ion batteries fade. To quantify such effects, capacity and resistance are usually tracked during battery lifetime. In this contribution, the RPT measurements described in Section II-B are used to assess capacity fade (ΔC) and resistance increase (ΔR) according to Eq. (1) and (2). The resistance used as representative measurement corresponds to DCIR at 50 % of SOC.

$$C_{RPT} = C_{RPT,0}(1 - \Delta C) \tag{1}$$

$$R_{RPT} = R_{RPT,0}(1 + \Delta R) \tag{2}$$

$C_{RPT,0}$ and $R_{RPT,0}$ are obtained from the RPT at the beginning of the test, i.e. of SL. The experimental results of the 16 cells under test (C1 to C16), together with their ageing conditions are gathered in Table I. State of Health ($SOH = C_{RPT}/C_N$) is also shown, as indicator of degradation from the fresh state.

Fig. 2 shows the results of ΔC and ΔR during the calendar ageing test for the conditions considered, classified according to T_{cal}. The complete test lasted 750 days, resulting in 25 RPTs measurements. When two samples were available, the average value of the results is kept.

As can be seen, increasing T_{cal} leads to an acceleration in the degradation rates of both parameters, in such a way that the tests at 60 °C had to be interrupted after 5 RPTs for security reasons, with up to 0.81 of ΔC (C13 and C14). Considering this RPT as a comparison point, ageing at 25 °C led to ΔC values below 0.03 (C4), while 45 °C resulted in a maximum fade of 0.18 (C8), which represented 27 and 4.5 times less than the capacity loss reported at the maximum T_{cal}, respectively. Regarding ΔR, storing at 60 °C increased up to 6.3 the initial measurement (C13 and C14), a value 5.9 times greater than the maximum increase reported at 25 °C, which was 1.07 (C4).

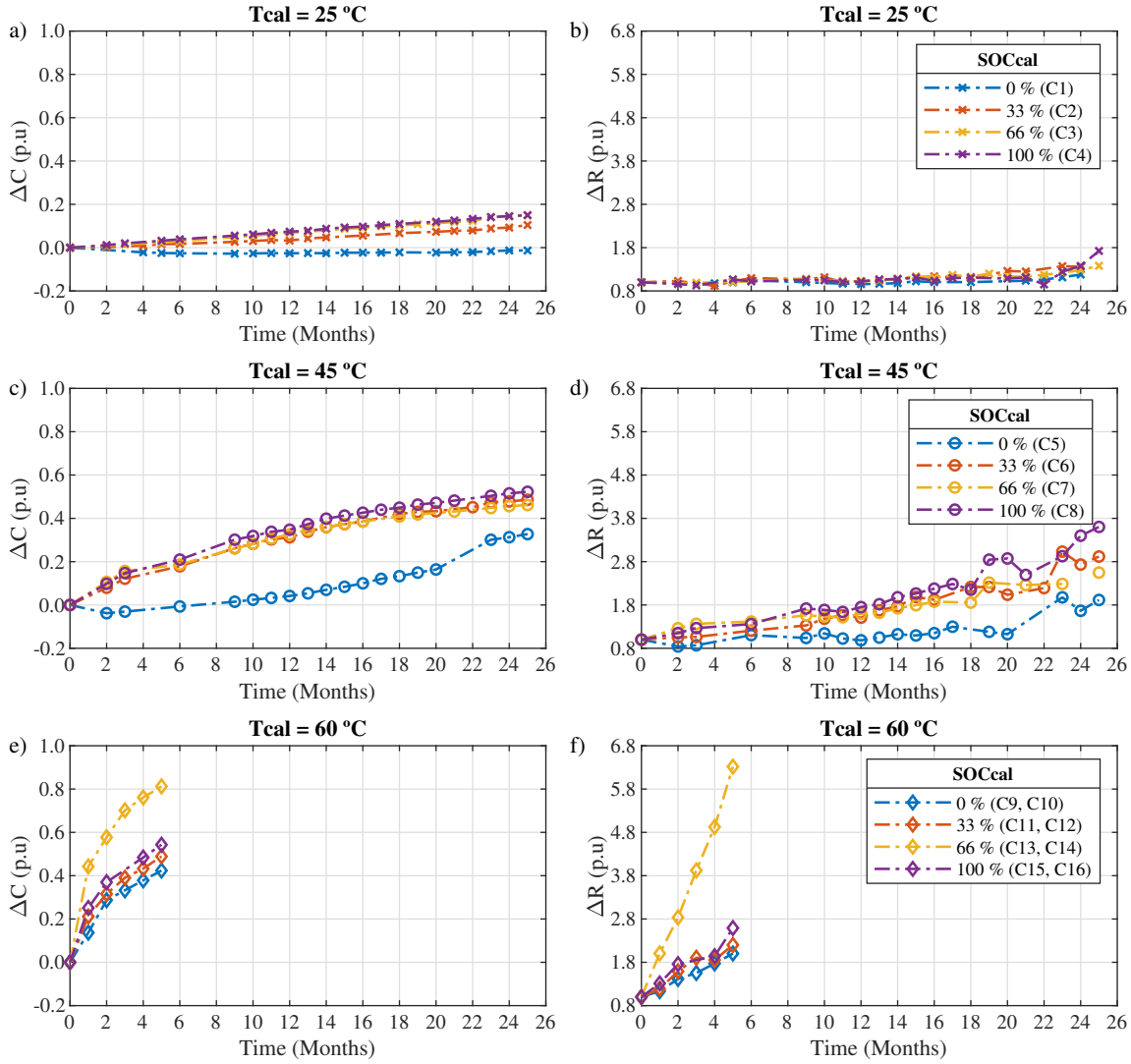

Fig. 2. Capacity fade and resistance increase at 25 ºC, 45 ºC and 60 ºC during the SL calendar ageing test.

For its part, storing at 45 °C was found to degrade DCIR with up to 1.4 of ΔR (C7).

On the other hand, for a given T_{cal}, in general degradation accelerates as SOC_{cal} rises. For example, at 45 °C, ΔC in the last RPT was 0.33 in C5, while C6, C7 and C8 lost 0.49, 0.46 and 0.52 of their initial capacity respectively. Considering ΔR, results showed an increase of 1.91, 2.92, 2.55 and 3.60 in C5, C6, C7 and C8 each. As an exception, at 60 °C, ageing with 66 % of SOC_{cal} is the fastest. This case has also been reported in other calendar ageing tests [9], [12], suggesting an increase of ΔC rate of LMO cells when stored at the lowest potential region of LMO as a possible reason [12].

Another aspect to be highlighted is the initial capacity increase and resistance decrease observed when storing at light conditions, more precisely at SOC_{cal} of 0 % at both 25 °C and 45 °C. Literature suggests as possible cause of this phenomena the flow of active Li from a passive anode region to the active part [10], [16]. This effect may last several days or months [10]. In this contribution, it is noticed to disappear after 5 months at 45 °C. However, at 25 °C it is observed during all the test.

Finally, it is important to note that the general ageing trends of ΔC and ΔR in the SL cells under test do not vary during the test. The degradation rate of Li-ion cells is determined by the main ageing mechanisms. Hence, it could be stated that in this test there was not a major change in such mechanisms. This is in good agreement with other calendar ageing results covering SL lifetime [9], and opposed to SL cycling ageing, in which an acceleration in ΔC and ΔR has been reported with similar cells [7]. After a general insight in the calendar ageing results, a deeper analysis on the influence of ageing factors such as temperature, SOC and time will be carried out in the next subsections.

TABLE I
CAPACITY AND RESISTANCE RESULTS AT THE BEGINNING OF THE TEST AND AGEING CONDITIONS OF THE SL CELLS

	RPT measurement			Ageing condition	
Cell	$C_{RPT,0}$ **(Ah)**	$R_{RPT,0}$ **(mΩ)**	**SOH** (%)	T_{cal} $(°C)$	SOC_{cal} **(%)**
C1	40.87	2.20	61.9	25	0
C2	40.20	2.35	60.9	25	33
C3	42.70	2.11	64.7	25	66
C4	43.41	2.25	65.8	25	100
C5	43.74	2.15	66.3	45	0
C6	44.16	2.25	66.9	45	33
C7	47.65	1.82	72.2	45	66
C8	47.65	2.02	72.2	45	100
C9	44.45	1.98	67.4	60	0
C10	44.44	2.12	67.3	60	0
C11	43.18	2.00	65.4	60	33
C12	43.83	2.14	66.4	60	33
C13	44.32	1.98	67.2	60	66
C14	44.38	1.94	67.2	60	66
C15	42.18	2.18	63.9	60	100
C16	42.10	2.05	63.8	60	100

IV. DEGRADATION ASSESSMENT AND MODELLING

The inhomogeneous ageing conditions during their usage in EVs, together with the dispersion in the internal parameters at the repurposing stage, motivate the assessment of calendar ageing in SL cells. Several questions arise, such as durability, how ageing factors affect SL or whether there is an acceleration in the ageing trends during lifetime. Thus, the influence of storage time, temperature and SOC is analysed in this section, and a degradation model is proposed and validated.

The first stage is data pre-processing. Measurement errors or abnormal behaviours such as decreasing ΔC values are left out of the analysis. After this step, 77.8 % of capacity measurements and 74.5 % of DCIR data from RPTs are kept. ΔC and ΔR are modelled as a product with two terms, as generally expressed in Eq. (3). On the one hand, *a(T,SOC)* gathers the influence of T_{cal} and SOC_{cal}, while storage time is considered as a power function with exponent β. Y is the variation of capacity or resistance.

$$\Delta Y = a(T, SOC)t^{\beta} \tag{3}$$

A. Influence of storage time

Time dependency of ΔC and ΔR are usually modelled as a power function, given by t^{β} in Eq. (3). The exact value of β varies with cell chemistry [11]. Fig. 3a) shows the results obtained for ΔC in the cells under test with the corresponding correlation coefficient. As can be seen, β ranges from 1.3 to 0.37, and therefore the selection of a unique value would be too imprecise. Considering other ageing factors, a similar behaviour depending on T_{cal} is observed. Thereby, the average value of β for each temperature is computed in both ΔC and ΔR expressions, and plotted in Fig. 3b). The evolution of β depending on T_{cal} is best fitted exponentially, as expressed in Eq. (4), with a coefficient of determination (Rsq) of 0.9980.

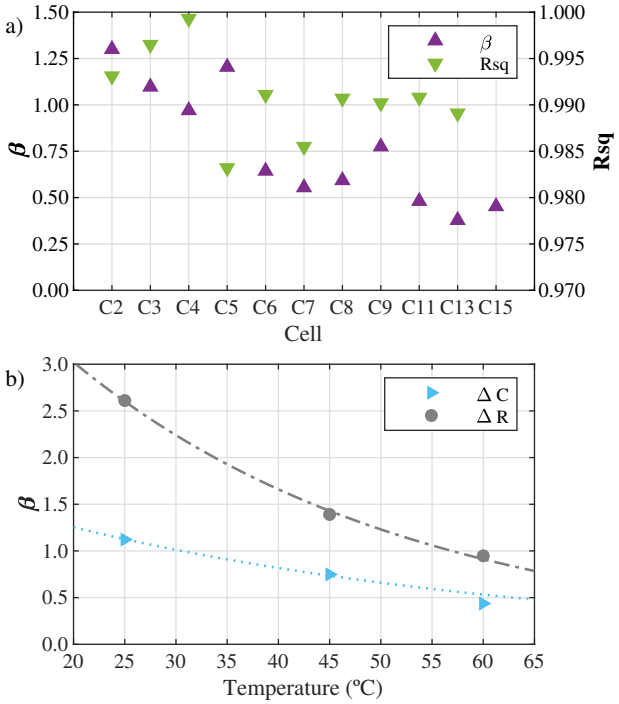

Fig. 3. a) Model exponent β for capacity fade and corresponding coefficient of determination Rsq for the SL cells and b) average value of β depending on temperature for capacity fade and resistance increase and exponential fitting.

The exact values of β_0 and β_1 are gathered in Table II.

$$\beta(T) = \beta_0 exp(\beta_1 T) \tag{4}$$

B. Influence of storage temperature

Temperature affects the reaction rates of chemical processes, in such a way that its rise leads to faster parasitic reactions, accelerating ΔC and ΔR. In order to quantify the impact of this parameter, the experimental data are fitted considering the three T_{cal} tested for a given SOC. In each case, the specific β is firstly computed from Eq. (3), and a_{Tcal} from Eq. (5) is then obtained.

$$a_{Tcal}(T) = a_0 exp(a_1 T) \tag{5}$$

Fig. 4 shows an example of the results obtained for 100 % SOC_{cal}. As can be seen, exponential fitting shows the best results, following Eq. (5), with Rsq values of 0.9996 in ΔC and 0.9999 in ΔR. This is in good agreement with Arrhenius's

TABLE II
COEFFICIENTS OF EQ.(3), (6) AND (7) FOR CAPACITY FADE AND RESISTANCE INCREASE SL MODELS

Coef.	ΔC	ΔR	**Coef.**	ΔC	ΔR
β_0	1.923	5.499	β_1	-2.139e-02	-2.994e-02
a_{00}	8.072e-05	1.809e-07	a_{10}	1.283e-01	2.308e-01
a_{01}	1.585e-05	2.166e-07	a_{11}	-9.512e-04	-1.730e-03
a_{02}	2.089e-03	2.854e-05	a_{12}	-1.934e-02	-1.533e-01
a_{03}	-5.991e-05	-8.537e-07	a_{13}	4.675e-03	1.315e-02
a_{04}	4.512e-07	6.392e-09	a_{14}	-3.490e-05	-9.810e-05

equation, which characterizes the change in reaction kinetics with temperature and is widely used in ageing models [10], [17].

C. Influence of storage SOC

Thermodynamic stability of electrolyte and electrodes have a direct impact on SEI growth [11]–[13], thus contributing to calendar degradation. This phenomena is adversely affected by a rise of storage SOC. However, the exact impact varies with cathode material and electrolyte composition [16]. It is difficult hence to define a common SOC dependency in Li-ion cells, and several alternatives are proposed in literature such as exponential [17] or lineal fitting [10].

In this contribution, once a_0 and a_1 were fitted for a given T_{cal}, their correlation with SOC_{cal} is examined. Fig. 5 shows the example of a_1. The influence of SOC_{cal} is found to be similar in ΔC and ΔR for both parameters. As can be seen, modelling SOC dependency requires considering two functions, and thereby Eq. (6) and (7) are proposed. The concrete values of fitting are shown in Table II.

$$a_0 = \begin{cases} a_{01}SOC + a_{00} & \text{if } SOC < 33\% \\ a_{04}SOC^2 + a_{03}SOC + a_{02} & \text{if } SOC > 33\% \end{cases} \quad (6)$$

$$a_1 = \begin{cases} a_{11}SOC + a_{10} & \text{if } SOC < 33\% \\ a_{14}SOC^2 + a_{13}SOC + a_{12} & \text{if } SOC > 33\% \end{cases} \quad (7)$$

D. Model results and validation

The proposed model, with Eq. (4), (5), (6) and (7), and the coefficients gathered in Table II is applied to the calendar ageing matrix conditions used in this contribution. In a second stage, the experimental results are compared to the estimations, and the corresponding Rsq is computed. Fig. 6a) shows the results of the capacity fade model. As can be seen, Rsq values range from 0.9206 (C1) to 0.9981 (C4), with an average value of 0.9875. This results are considered satisfactory, and slightly over other SL calendar ageing modelling approaches such as [9], whose average fitting was 0.9722, with a T_{cal} range from 40 °C to 55 °C. It should be noted that [9] analysed LFP cells and therefore the specific ageing of the chemistry may influence the comparison. On the other hand, resistance increase modelling show a fitting accuracy from 0.8441 (C4) to 0.9944 (C13), with an average value of 0.9389, as plotted in Fig. 6b). Given the greater sensitivity of this parameter to measurement errors, the results are also considered as satisfactory. For its part, [9] considers power fade, reaching an average value of 0.9507.

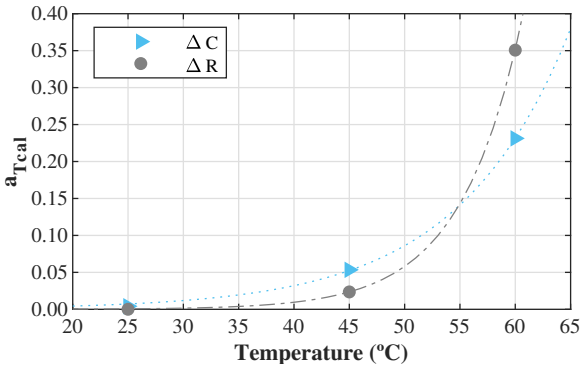

Fig. 4. Temperature factor for capacity fade and resistance increase and corresponding fitting.

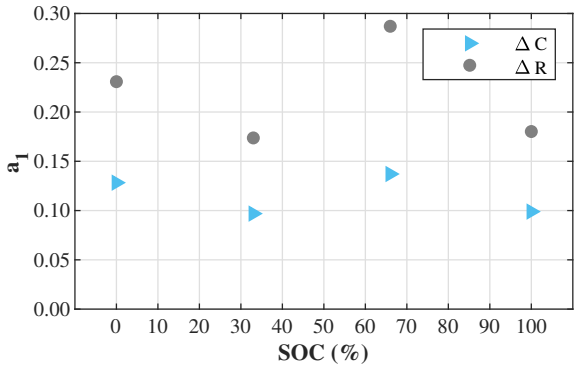

Fig. 5. SOC dependency of the fitting coefficient a_1 for capacity fade and resistance increase cases.

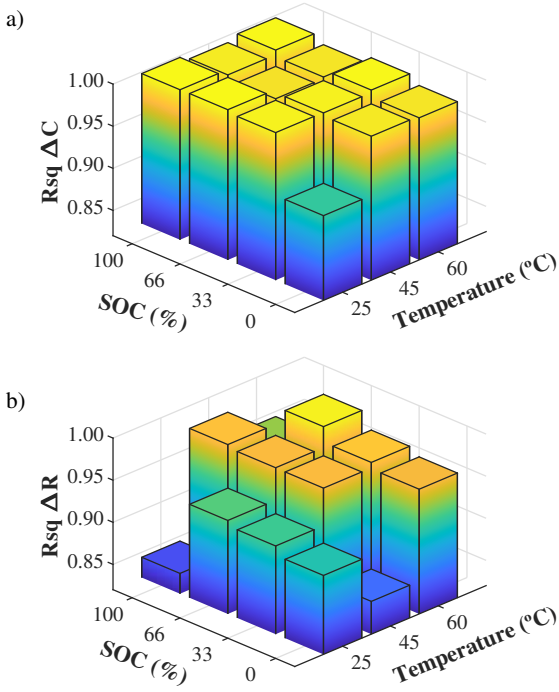

Fig. 6. Fitting error Rsq of the proposed model for capacity fade and resistance increase in the calendar ageing conditions tested.

TABLE III
VALIDATION RESULTS OF THE PROPOSED CALENDAR AGEING MODEL IN SL CELLS

Cell	C10	C12	C14	C16
$\Delta C_{RPT,5}$ (p.u.)	0.40	0.51	0.80	0.55
$\Delta R_{RPT,5}$ (p.u.)	1.92	2.38	5.99	2.35
Rsq Δ_C	0.9999	0.9995	0.9941	0.9957
Rsq Δ_R	0.9974	0.9557	0.9916	0.9700

In a second stage, four SL cells are stored at 60 °C under the different SOC_{cal} considered (C10, C12, C14, C16). As in the model data set, the ageing tests were stopped after 5 months for security reasons. At the end of the test, the initial capacity faded from 0.40 (C10) to 0.80 (C14), as shown in Table III, and resistance increased from 0.67 (C10) to 4.99 (C14) SOC_{cal} of 66% is found to be the most aggressive, which confirms the previous experimental results.

Goodness of fitting is evaluated through Rsq, being the results presented in Table III. As can be seen, ΔC is accurately estimated, with Rsq values over 0.9941. Resistance increase prediction is also satisfactory, with Rsq values above 0.9557. The selected T_{cal} leads to a very fast degradation, in which the internal dispersion and EV ageing history of the cells may be compounded. For example, comparing C13 and C14, with similar initial capacity and DCIR values, they lost almost equal capacity (0.82 and 0.80 respectively), while ΔR was much greater in C13 than C14 (6.62 vs. 5.99). In view of the accuracy results, it is concluded that the proposed model is able to handle with this inhomogeneous ageing.

V. CONCLUSION

This contribution assesses calendar ageing behaviour of reused cells from EVs. The need of studying degradation to ensure technical and economic viability of SL batteries, together with the research gap found in this field motivates the analysis.

A total of 16 Nissan Leaf cells are experimentally aged, at three temperatures (25, 45 and 60 °C) and four SOC levels (0, 33, 66 and 100 %). After 750 days of testing, the SOH of the cells ranged from 72.2 % to 13 %, thereby covering a wide SL lifetime. At a first stage, the influence of temperature and SOC is analysed. In general, increasing these factors accelerates degradation. The impact of temperature is found to be specially important, with capacity fade up to 27 times greater at 60 °C than at 25 °C, and resistance increase almost 6 times larger. On the other hand, for a given temperature, 45 °C, SOC is found to almost double capacity loss and resistance increase at 100 % with respect to 0 %. Its influence is best fitted by a polynomial expression. The degradation rates are found to be constant over SL lifetime, being the worst ageing conditions 60 °C and 66 % of SOC. The proposed model is fitted to the experimental results, and validated by means of four extra cells stored at 60 °C at the different SOC levels. Validation results show Rsq of 0.9941 in terms of capacity fade and 0.9557 in resistance increase. The hetererogeneous ageing of the SL cells is thus well tracked by the model.

Overall, this contribution reinforces the ageing assessment of SL batteries, thereby contributing to their technical and economic viability. As future lines of this work, a similar study considering cycling ageing and its stress factors is encouraged.

REFERENCES

[1] International Energy Agency, "Global EV Outlook 2021", IEA, Paris.

[2] E. Martinez-Laserna et al., "Battery second life: Hype, hope or reality? A critical review of the state of the art", Renewable and Sustainable Energy Reviews, vol. 93, 2018, pp. 701-718.

[3] A. Podias, et al., "Sustainability Assessment of Second Use Applications of Automotive Batteries: Ageing of Li-Ion Battery Cells in Automotive and Grid-Scale Applications", World Electr. Veh. J, 2018, vol. 9, p. 24, doi: 0.3390/wevj9020024

[4] C. Curry, "Lithium-ion Battery Costs and Market", Bloomberg New Energy Finance, July 2017.

[5] E. Braco, I. S. Martín, A. Berrueta, P. Sanchis and A. Ursúa, "Experimental Assessment of First- and Second-Life Electric Vehicle Batteries: Performance, Capacity Dispersion, and Aging," in IEEE Transactions on Industry Applications, vol. 57, no. 4, pp. 4107-4117, July-Aug. 2021, doi: 10.1109/TIA.2021.3075180.

[6] Y. Zhang et al., "Performance assessment of retired EV battery modules for echelon use," Energy, vol. 193, p. 116555, 2020, doi: 10.1016/j.energy.2019.116555.

[7] E. Braco, I. San Martín, A. Berrueta, P. Sanchis, and A. Ursúa, "Experimental assessment of cycling ageing of lithium-ion second-life batteries from electric vehicles," Journal of Energy Storage, vol. 32, no. July, p. 101695, 2020, doi: 10.1016/j.est.2020.101695.

[8] C. White, B. Thompson, and L. G. Swan, "Repurposed electric vehicle battery performance in second-life electricity grid frequency regulation service," Journal of Energy Storage, vol. 28, no. January, p. 101278, 2020, doi: 10.1016/j.est.2020.101278

[9] M. Swierczynski, D. -I. Stroe and S. K. Kær, "Calendar ageing of LiFePO4/C batteries in the second life applications," 2017 19th European Conference on Power Electronics and Applications (EPE'17 ECCE Europe), 2017, pp. P.1-P.8, doi: 10.23919/EPE17ECCEEurope.2017.8099173.

[10] A. Krupp, R. Beckmann, T. Diekmann, E. Ferg, F. Schuldt, C. Agert, "Calendar aging model for lithium-ion batteries considering the influence of cell characterization", Journal of Energy Storage, vol. 45, 2022, p. 103506, doi: 10.1016/j.est.2021.103506

[11] M. Dubarry, N. Qin, P. Brooker "Calendar aging of commercial Li-ion cells of different chemistries – A review", Current Opinion in Electrochemistry, vol. 9, 2018, pp. 106-113, doi: 10.1016/j.coelec.2018.05.023.

[12] S.-H Wu, P.-H. Lee, "Storage fading of a commercial 18650 cell comprised with NMC/LMO cathode and graphite anode", Journal of Power Sources, vol. 349, 2017, pp. 27-36, doi: 10.1016/j.jpowsour.2017.03.002.

[13] C. Geisbauer, K. Wöhrl, C. Mittmann, H.-G. Schweiger, "Review—Review of Safety Aspects of Calendar Aged Lithium Ion Batteries", Journal of The Electrochemical Society, vol. 167, 2020, p. 090523, doi: 10.1149/ 1945-7111/ab89bf

[14] A. Eddahech, O. Briat, J.-M. Vinassa, "Performance comparison of four lithium–ion battery technologies under calendar aging", Energy, vol. 84, 2015, pp. 542-550, doi: 10.1016/j.energy.2015.03.019.

[15] E. Braco, I. S. Martin, A. Ursúa and P. Sanchis, "Incremental capacity analysis of lithium-ion second-life batteries from electric vehicles under cycling ageing," 2021 IEEE International Conference on Environment and Electrical Engineering and 2021 IEEE Industrial and Commercial Power Systems Europe (EEEIC / I&CPS Europe), 2021, pp. 1-6, doi: 10.1109/EEEIC/ICPSEurope51590.2021.9584637.

[16] M. Lewerenz, G. Fuchs, L. Becker, D. U. Sauer, "Irreversible calendar aging and quantification of the reversible capacity loss caused by anode overhang", Journal of Energy Storage, v. 18, 2018, pp. 149-159, doi: 10.1016/j.est.2018.04.029.

[17] S. -I. Stroe, M. Swierczynski, S. K. Kær and R. Teodorescu, "Degradation Behavior of Lithium-Ion Batteries During Calendar Ageing—The Case of the Internal Resistance Increase," IEEE Transactions on Industry Applications, vol. 54, no. 1, pp. 517-525, 2018, doi: 10.1109/TIA.2017.2756026.